Journal of Ethnopharmacology 211 (2018) 285–294

Contents lists available at ScienceDirect

Journal of Ethnopharmacology

journal homepage: www.elsevier.com/locate/jethpharm

Anti-proliferative and pro-apoptotic effects of *Uncaria tomentosa* aqueous extract in squamous carcinoma cells

Francesca Ciani[a,*,1], Simona Tafuri[a,1], Annaelena Troiano[b], Alessio Cimmino[c], Bianca Saveria Fioretto[b], Andrea Maria Guarino[b], Alessandra Pollice[b], Maria Vivo[b], Antonio Evidente[c], Domenico Carotenuto[d], Viola Calabrò[b,*]

[a] Department of Veterinary Medicine and Animal Productions, University "Federico II", Via Veterinaria 1, Naples 80137, Italy
[b] Department of Biology, Complesso Universitario Monte S. Angelo, University "Federico II", Via Cintia, Monte S. Angelo, Naples 80126, Italy
[c] Department of C hemical Sciences, University "Federico II", Complesso Universitario Monte S. Angelo, Via Cintia,Monte S. Angelo, Naples 80126, Italy
[d] UNMSM, Universidad Nacional Mayor San Marcos, Lima, Peru

ARTICLE INFO

Keywords:
Squamous carcinoma
Cat's claw
Y box binding protein 1
Oxidative stress
Cell death

ABSTRACT

Uncaria tomentosa (Willd.) DC. (Rubiacee), also known as *uña de gato*, is a plant that grows wild in the upper Amazon region of Peru and has been widely used in folk medicine to treat several health conditions including cancer. We have produced an aqueous extract from *Uncaria tomentosa* (UT-ex) and analyzed its effects on squamous carcinoma cells and immortalized HaCaT keratinocytes. Squamous cell carcinoma (SCC) is an uncontrolled growth of abnormal cells arising in the skin's squamous layer of epidermis. When detected at an early stage, SCCs are almost curable, however, if left untreated, they can penetrate the underlying tissue and become disfiguring. We have evaluated cell proliferation, apoptosis and the level of reactive oxygen species following UT-ex treatment. UT-ex affected cell cycle progression and reduced cell viability in a dose and time-dependent manner. From a mechanistic point of view, this delay in cell growth coincided with the increase of reactive oxygen species (ROS). Furthermore, PARP1 cleavage was associated to the reduction of Y-box binding protein 1 (YB-1) 36 kDa, a nuclear prosurvival factor involved in DNA damage repair. These data indicate that UT-ex-induced cell death can be ascribed, at least in part, to its ability both to induce oxidative DNA damage and antagonize the mechanism of DNA repair relying upon YB-1 activity. They also show that non metastatic SCCs are more susceptible to UT-ex treatment than untransformed keratinocytes supporting the use of UT-ex for the treatment of precancerous and early forms of squamous cell carcinomas. Preliminary chemical investigation of UT-ex revealed the presence of hydrophilic low-medium molecular weight metabolites with anticancer potential towards squamous carcinoma cells.

1. Introduction

Squamous cell carcinoma (SCC) is an uncontrolled growth of abnormal cells arising in the squamous cells, which compose most of the skin's upper layers (Sapijaszko et al., 2015). SCCs may occur on any part of the body, including the mucous membranes and genitals, but are most common in areas frequently exposed to the sun, such as the neck, face, balding scalp, arms and legs. Squamous cell carcinomas detected at an early stage are almost always curable. However, left untreated, they eventually penetrate the underlying tissues and can become disfiguring. A small percentage may even metastasize to local lymph nodes, distant tissues, and organs and can become fatal. Actinic keratoses (AKs) are considered the earliest form of SCC and may be the first sign of squamous cell carcinoma (Boukamp, 2005); indeed, 40–60% of squamous cell carcinomas begin as untreated AKs.

Though considerable progress has been made in developing effective skin cancer treatments, surgery and radiation are still predominant and it would be beneficial to find new topical treatments for precancerous skin lesions to prevent their progression.

Nowadays, there is an increased demand for alternative concepts or approaches to cancer treatment. Compelling evidence from epidemiological and experimental studies highlight the importance of compounds derived from plants, "phytochemicals", for inhibiting the development and spread of tumors in pre-clinical studies.

Uncaria tomentosa (Willd.) DC., from the Rubiaceae family, is a thorny liana that grows wild in the upper Amazon region of Peru and

* Corresponding authors.
E-mail addresses: francesca.ciani@unina.it (F. Ciani), vcalabro@unina.it (V. Calabrò).
[1] These authors contributed equally to this work.

http://dx.doi.org/10.1016/j.jep.2017.09.031
Received 14 June 2017; Received in revised form 21 September 2017; Accepted 24 September 2017
Available online 28 September 2017
0378-8741/

neighboring countries. In Peru, *Uncaria tomentosa*, also known as *uña de gato*, is believed to have anti-inflammatory and anti-tumoral properties (Heitzman et al., 2005; Garcia Prado et al., 2007). The boiled extract of *Uncaria tomentosa* root/bark has been used over the centuries by the indigenous civilization of the Amazonian rain forest for the treatment of fever, rheumatism, arthritis, gastrointestinal disorders, cirrhosis, neurodegenerative diseases, microbial infections, cancer, skin impurities and inflammation (Keplinger et al., 1998; Ccahuana-Vasquez et al., 2007).

Many active compounds have been isolated from *Uncaria tomentosa* including antioxidants such as tannin, catechins, and procyanidins, sterols, triterpenes, flavonoids, carboxyl alkyl esters, indol and oxindol alkaloids (Heitzman et al., 2005; Wagner et al., 1985a). In particular, alkaloids, the major active components of Uncaria species were extensively studied for their potential use as anticancer agents and found to be effective against the proliferation of breast and bladder tumor lineages (Riva et al., 2001; Kaiser et al., 2013). From a mechanistic point of view, *Uncaria tomentosa* was found to affect tumor growth by inhibiting the Wnt or NF-kB/TNFα signaling pathways (Akesson et al., 2003; Gurrola-Diaz et al., 2011). Moreover, *Uncaria tomentosa* aqueous extract was reported to enhance DNA repair in human skin organ cultures irradiated with UV-B (Mammone et al., 2006) and to abate actinic keratoses and early squamous cell cancer in hairless mice exposed to UV-A radiation thereby suggesting its possible application as a product for skin cancer protection (Mentor et al., 2015).

The aim of the present study was to analyze, the biological effects of *Uncaria tomentosa* extract on human immortalized keratinocytes and squamous carcinoma cells in order to provide molecular evidence supporting its therapeutic use against this type of cancer.

2. Materials and methods

2.1. Cell culture and reagents

HaCaT, spontaneously immortalized keratinocytes from adult skin, were purchased from Service Cell Line (CLS, Germany) and cultured as described (Amoresano et al., 2010); A431, human epidermoid carcinoma cells were from American Type Culture Collection (ATCC, Manassas, VA). Head and neck cancer cell lines SCC011, SCC013 and SCC022 were originally derived from tumors in patients affected by squamous cell carcinoma of the upper aerodigestive tract (Resto et al., 2008). HaCaT and A431 cell lines were cultured in Dulbecco's Modified Eagle's Medium (DMEM, Sigma Chemical Co, St. Louis, MO, USA), while all SCC lines were cultured in Roswell Park Memorial Institute medium (RPMI 1640 Sigma Chemical Co, St. Louis, MO, USA). All cell line cultures were supplemented with 10% fetal bovine serum (FBS, Hyclone Laboratories, Inc., Logan, UT, USA), 1% L-glutamine, and 1% penicillin-streptomycin (ICN Biomedicals, Inc., Aurora, OH, USA) at 37 °C in humidified atmosphere of 5% CO_2.

2.2. Bright-field microscopy

HaCaT, A431, SCC011, SCC013 and SCC022 cells were plated at a density of 2.5×10^5 per well and treated with the indicated doses of Uncaria Tomentosa. After 24 h of treatment, images were acquired in phase-contrast at Nikon Eclipse TE-2000U.

2.3. Antibodies

The primary antibodies GAPDH (6C5), actin (I-19) and actinin (H-2) were purchased from Santa Cruz Biotechnology, Inc. Santa Cruz, CA, USA). Primary antibodies YB-1 (ab12148), hnRNPA1 (ab177152) were from Abcam (Cambridge, UK). PARP1, p21-WAF (12D1), Bax (D2E11) and H2AX antibodies were from Cell Signaling (Beverly, MA). Anti-Ubiquitin antibodies were purchased from DAKO (Glostrup, Denmark).

2.4. Extract preparation

The water extract of *Uncaria tomentosa* bark (UT-ex) used for the experiments was prepared as follows: 15 g of dried bark were shredded and boiled for 30 min in 500 ml of bi-distilled H_2O, then cooled at room temperature (RT) and filtered through sterile gauze. The concentration (w/v) was estimated by the ratio between the weight of the bark, expressed in grams, and the final volume obtained at the end of the preparation:

$$15\ g/400\text{ml} = [00.0375\ g/\text{ml}]$$

UT-ex contains 1.28 mg/ml of proteins as determined by Bradford assay, 3.08 mg/ml phenols and 4.05 mg/ml carboidrates (2.08 pentoses and 1.97 hexoses).

The water extract was filtered through a 0.20 μm filter before being applied to the cells. An aliquot was lyophilized (SAVANT, SC110 Speed Vac Plus A) and resuspended in the initial volume of sterile H_2O in order to check for loss of properties during the sublimation process (ReUT-ex).

2.5. Cell viability assay

The effect of *Uncaria tomentosa* on cell viability was evaluated by measuring the reduction of 3-(4,5-dimethylthiazol-2) 2,5-diphenyltetrazolium bromide (MTT) to formazan by mitochondrial dehydrogenase. Briefly, 9×10^3 cells were seeded on 96-well plates and exposed to increasing concentrations of *UT-ex* (from 0.3 to 10 mg/ml) for 24, 48 and 72 h. MTT/PBS solution (0.5 mg/ml) was then added to the wells and incubated for 3 h at 37 °C in a humidified atmosphere. The reaction was stopped by removal of the supernatant followed by dissolving the formazan product in acidic isopropanol. Optical density was measured with an ELISA reader (Bio-Rad) using a 570 nm filter. Under these conditions, undissolved formazan crystals were not observed. Cell viability was assessed comparing optical density of the treated samples compared to the control group.

2.6. Cell growth profile

HaCaT, A431 and SCC022 cells were plated at a density of 2.5×10^5 per well in a Corning 6 well plate and the counts were performed in a Neubauer chamber by Trypan Blue dye exclusion. Briefly, 20 μL cell suspension was diluted 1:1 with 0.4% solution of trypan blue in phosphate saline buffer pH 7.2. Cell counting was carried out at 24-hr intervals for 3 days.

2.7. Cell cycle analysis

Cells were seeded at 3×10^5 in 35 mm dishes and treated with UT-ex at 0.3 and 1.5 mg/ml for 24 h. Cells were then trypsinized and washed by centrifugation (1200 rpm, 4 min, 4 °C) in Phosphate Buffered Saline (PBS 1x). The cell pellet was resuspended in methanol, incubated in ice for 20 min and centrifuged at 1200 rpm, 5 min, 4 °C. After a wash in PBS, the cell pellet was incubated in PBS 1x, containing RNase 100 μg/ml for 20 min at RT. Propidium iodide was then added at a concentration of 50 μg/ml for 30 min at 4 °C. Cell cycle analysis was performed on the BD Accury™ C6 flow cytometer (BD Biosciences). Cell debris and aggregates were excluded from the analysis.

2.8. Western blot and immunoprecipitation analyses

Immunoblots (IB) and immunoprecipitations (Co-IP) were performed as previously described (Calabrò et al., 2004; Di Costanzo et al., 2011). *Uncaria tomentosa* treated and untreated cells were harvested in lysis buffer (50 mM Tris-HCl pH 7.5, 5 mM EDTA, 150 mM NaCl, 1% NP-40, 1 mM phenylmethylsulfonyl fluoride, 0.5% sodium deoxycholate, and protease inhibitors) as previously described (Lo Iacono

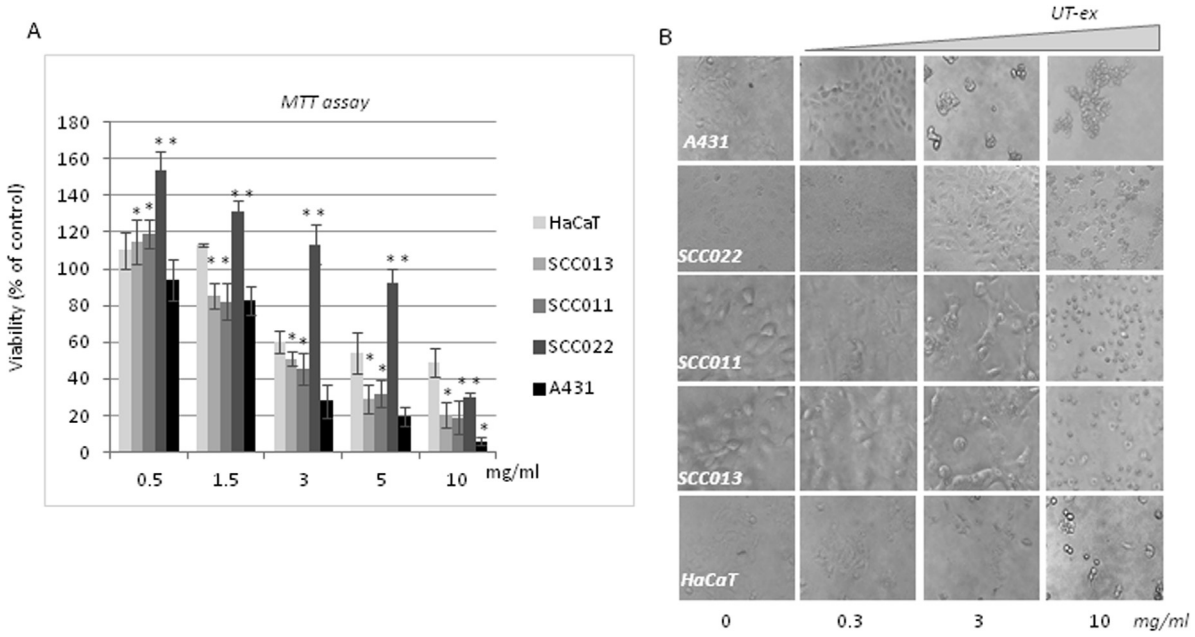

Fig. 1. (**A**) Percentage of viability of HaCaT, SCC013, SCC011, SCC022 and A431 cell lines after 48 h of incubation with the indicated doses of UT-ex (mg/ml). Cell viability was measured by the chromogenic MTT assay and is expressed as the percentage of viable cells compared to cells in the absence of the plant extract (mean ± S.D. n = 6 technical replicates). ANOVA * $p < 0.05$, ** $p < 0.005$. (**B**) Bright-field microscopy of representative images of A431, SCC022, SCC011, SCC013 and HaCaT cells after 24 h of incubation with UT-ex at increasing concentrations from 0 to 10 mg/ml (0, 0.3, 3.0 and 10 mg/ml).

et al., 2006). Total cell lysates were incubated on ice for 40 min and clarified by centrifugation at 13,200 rpm for 15 min at 4 °C. The amount of protein in the samples was determined by the Bio-Rad protein assay (Bio-Rad, Milan, Italy). After the addition of Laemmli buffer (Sigma Chemical Co, St. Louis, MO, USA) the samples were boiled at 100 °C for 5 min and resolved by SDS-polyacrylamide gel electrophoresis (SDS-PAGE). The proteins were then transferred to a polyvinylidene difluoride membrane (PDVF, Millipore) using a Mini transblot apparatus (Bio-Rad, Milan, Italy) according to manufacturer's instructions. The PVDF membrane was blocked in 5% w/v milk buffer (5% w/v non-fat dried milk, 50 mM Tris, 200 mM NaCl, 0.2% Tween 20) and incubated with primary antibodies diluted in 5% w/v milk or bovine serum albumin (BSA) buffer for 2 h at RT or overnight at 4 °C. The blots, washed three times with TTBS (Tris-buffered saline, 0.1% Tween), were incubated for 1 h at RT with HRP-conjugated secondary antibodies (Santa-Cruz biotechnology). The proteins were visualized by an enhanced chemiluminescence method (ECL, GE-Healthcare) and analyzed by Quantity One W software of ChemiDoc TM XRS system (Bio-Rad, Milan, Italy). For IP experiments, extracts were pre-cleared with 30 µL of protein A-agarose (50% slurry; Roche, Manheim, Germany), and incubated overnight at 4 °C with anti-YB-1 (3 µg) or α-rabbit IgG (3 µg). Whole extracts were separated by SDS-PAGE and subjected to immunoblot, as previously described.

2.9. Reactive oxygen species (ROS) generation assay

Intracellular ROS generation was measured by flow cytometry using 2′−7′ dichlorofluorescein diacetate (DCFDA), a non-fluorescent compound permeable to the cell membrane, which can be oxidized by ROS, giving a fluorescent compound. In brief, 3×10^5 cells were treated with different concentrations of *Uncaria tomentosa* (0.3 and 3 mg/ml), the medium was removed after 24 h and cells were washed with PBS. Fresh medium with DCFDA (1 mM) was added for 30 min, then DCFDA was removed by washing in PBS and the cells were harvested. The measurement of ROS was obtained using flow cytometry Accuri C6 (BD-biosciences, US) and for each sample at least 10, 000 events were evaluated. The fluorescence emitted from the cells treated with DCFDA, compared to the untreated cells, was performed using the FL1-A (530–533 nm) channel. The data obtained as mean fluorescence intensities were analyzed and converted into percentages of ROS by BD Accuri C6 Software.

2.10. Genomic DNA extraction

Uncaria tomentosa treated and untreated cells were harvested in lysis buffer (10 mM Tris pH 8.0, 50 mM NaCl, 20 µg/ml di Proteasi K, 20 µg/ml di RNasi) with 1% SDS. Samples were incubated 2 h at 55 °C and then treated with 1.5 M of NaCl. A 1:1 vol of chloroform was added and samples were incubated for 1 h on rotation at room temperature. Samples were centrifuged at 13,200 rpm for 3 min, then 0.7 vol (compared to volume of lysis buffer) of isopropanol was added to supernatants.

Samples were centrifuged for 3 min at 13,200 rpm, the white pellet was resuspended in TE solution. 20 microliters of each sample were loaded in 1.2% agarose gel in TAE buffer. Images were acquired after trans-UV irradiation and analyzed by Quantity One W software of ChemiDoc TM XRS system (Bio-Rad, Milan, Italy).

2.11. Comet assay

The glass slides were coated with 50 µL of normal-melting-point agarose (0.7%). Then, 200 µL of 1% agarose were applied and allowed to solidify at 4 °C. Then, 50 µL of cell/agarose mixture, 25 µL of 0.7% agarose plus 25 µL of cell suspension (10^5 cells), was applied as a third layer. After 20 min in ice, 200 µL of 0.7% agarose was applied as a cover layer of the microgel.

The slides were immersed in cold fresh lysis solution (2.5 M NaCl, 100 mM EDTA, 10 mM Tris) for 1.5 h at 4 °C and then placed for 20 min in electrophoresis buffer (300 mM NaOH, 1 mM EDTA, pH 13). The electrophoresis was performed at 25 V at room temperature for 30 min. The slides were then rinsed twice with the neutralization buffer (0.4 M Tris, pH 7.5) and stained with DAPI.

Images were acquired with Nikon Eclipse TE-2000U fluorescence microscope. Cells (100) were counted and those showing the comet were expressed as percentage of the total.

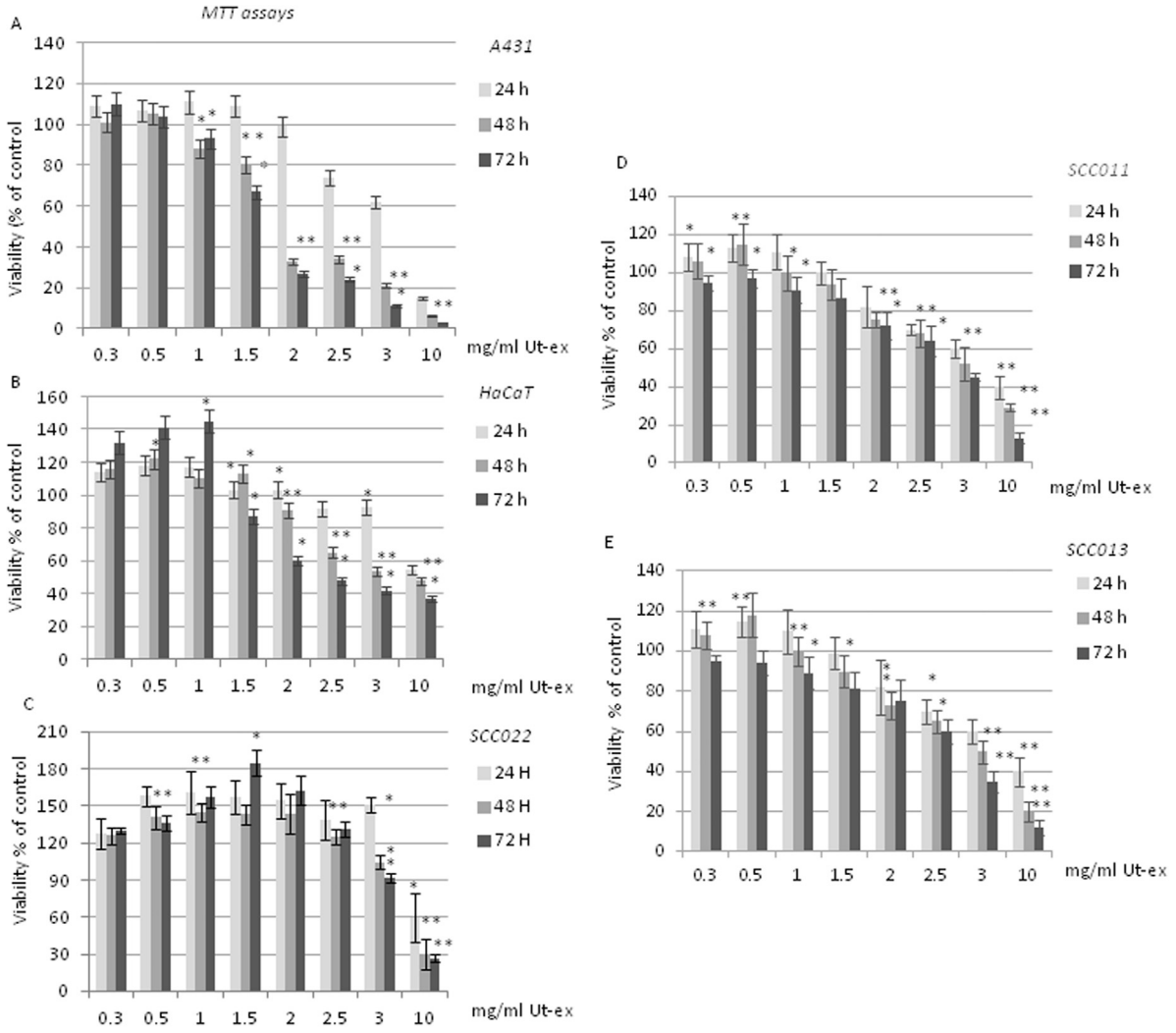

Fig. 2. (**A–E**) Percentage of viability of A431, HaCaT, SCC022, SCC011 and SCC013 cells after 24, 48 and 72 h of incubation with increasing doses of UT-ex (0.3, 0.5, 1, 1.5, 2, 2.5, 3.0 and 10 mg/ml). Cell viability was measured by the chromogenic MTT assay and is expressed as the percentage of viable cells compared to cells in the absence of the plant extract (mean ± S.D. n = 6 technical replicates). ANOVA * $p < 0.05$, ** $p < 0.005$.

2.12. Statistical analysis

Statistical significance of difference in measured variables between control and treated groups was determined by *t*-test or one-way ANOVA. Difference was considered significant at $P < 0.05$ (*) and $P < 0.005$ (**).

2.13. General chemical procedures

Analytical and preparative TLC were performed on silica gel (Kieselgel 60, F_{254}, 0.20 and 0.5 mm respectively) and on reversed phase (Kieselgel 60 RP-18, F_{254}, 0.20 mm) plates (Merck, Darmstadt, Germany). The spots were visualized by exposure to UV radiation (254), or by spraying first with 10% H_2SO_4 in MeOH and then with 5% phosphomolybdic acid in EtOH, followed by heating at 110 °C for 10 min.

The HPLC system (HITACHI) consisted of a pump (5160) and a spectrophotometric detector (5410). The HPLC separation were performed using a Phenomenex LUNA (C18 (2) 5 u 150 × 4.6 mm). The mobile phase used to elute the samples was MeOH:H_2O, 0.1% TFA at a flow rate of 0.4 ml/min. The analysis was performed using a linear gradient starting from 30% of MeOH increased linearly to 50% MeOH in 10 min and holded this conditions for 25 min. The initial conditions were restored according to a linear gradient over 5 min and the column was re-equilibrated under these conditions for 10 min before the next run. Detection was performed at 250 nm. Samples were injected using a 20-μL loop and monitored for 30 min.

^{1}H NMR spectra were recorded at 400 or 500 MHz in CDCl3 on Bruker (Karlsruhe, Germany) and Varian (Palo Alto, CA, USA). The same solvent was used as internal standard.

LC-TOF analysis were performed using the LC/MS TOF system (AGILENT 6230B, HPLC 1260 Infinity), using the same HPLC conditions.

Spectra/Por Dyalisis Membrane (cut-off 3500 Da) were purchased from Sigma (Milan, Italy) and the dialyses carried out for two days against a large volume of distilled water.

3. Results

3.1. UT-ex cytotoxicity in squamous carcinoma cells

Human immortalized HaCaT keratinocytes and keratinocyte-derived squamous carcinoma cells (SCC013, SCC011, SCC022 and A431) were treated for 48 h with increasing doses of UT-ex, from 0.5 to 10 mg/ml, and cell viability was analyzed by MTT assay. The yellow tetrazolium salt 3-(4, 5-dimethylthiazol-2-yl) − 2, 5-diphenyltetrazolium bromide (MTT) is widely used to determine cell viability in cell proliferation and cytotoxic assays. MTT is reduced by metabolically

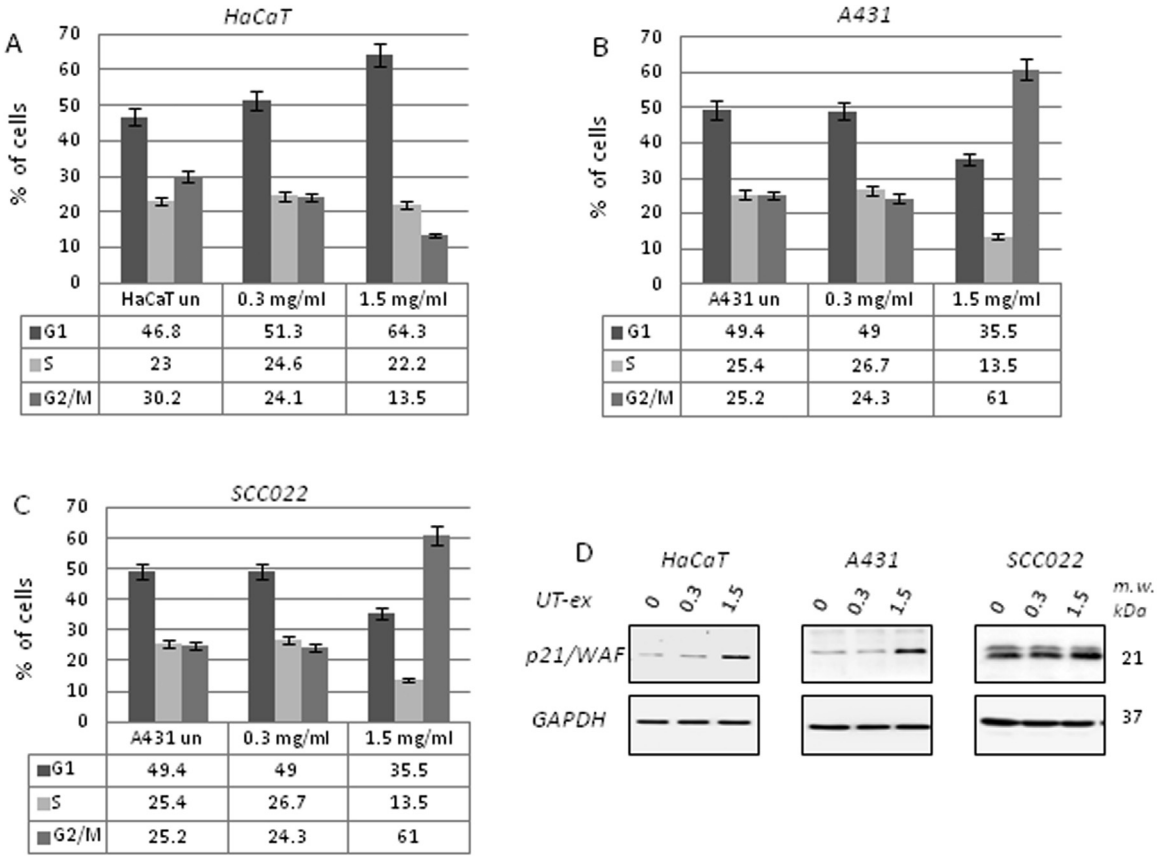

Fig. 3. Cell cycle analysis of HaCaT (**A**), A431 **(B)** and SCC022 (**C**) cells treated or not with 0.3 and 1.5 mg/ml of UT-ex. Each plot represents the percentage of cells in the different cell cycle phases. (**D**) Immunoblot analysis of extracts from HaCaT, A431 and SCC022 cells treated with 0.3 and 1.5 mg/ml of UT-ex for 24 h. Aliquots of extracts (25 µg) were loaded and subjected to SDS-PAGE and immunoblot analysis with p21-WAF and GAPDH antibodies.

active cells to form an insoluble purple formazan product that is quantifiable by spectrophotometry. At 0.5 mg/ml of UT-ex, immortalized HaCaT, highly metastatic SCC022, and non-metastatic SCC013 and SCC011 cells were more viable than control cells (ranging from 1.1 to 1.5 folds) (Fig. 1A). Vulvar epidermoid A431 cells remained almost unaffected by treatment with 0.5 mg/ml of UT-ex (Fig. 1A). At higher concentrations, UT-ex was clearly cytotoxic and exhibited a dose-dependent effects in all tested cell lines (Fig. 1A). Compared to untreated controls, epidermoid A431 cells were the most susceptible to UT-ex with a residual cell viability of less than 10% at 10 mg/ml of UT-ex (Fig. 1A).

Bright-field microscopy and imaging confirmed the major sensitivity of A431 cells compared to the other cell lines. However, upon treatment with 10 mg/ml of UT-ex, all tested cells exhibited a round morphology, a cytoplasmic vacuolization and loss of cell-cell contacts, indicating severe cell damage (Fig. 1B).

To better examine their different susceptibility, we performed a more detailed evaluation of UT-ex, cytotoxicity on squamous cancer cell lines compared to spontaneously immortalized HaCaT keratinocytes. We confirmed that A431 cells were the most sensitive to UT-ex with a half-maximal inhibitory concentration (IC_{50}) between 1.5 and 2.0 mg/ml at 48 h of treatment (Fig. 2A). HaCaT cell viability began to progressively decline at UT-ex concentration of 1.5 mg/ml of UT-ex, (Fig. 2B) while viability of SCC022, SCC011 and SCC013 cells dropped precipitously to 20–30% upon treatment with 10 mg/ml of UT-ex for 48 h (Fig. 2C–E). As shown in Fig. 2A–E, the reduction of cell viability was most pronounced at 48 and 72 h of treatment in all cell lines thus revealing a time-dependent toxicity of UT-ex. Remarkably, at 10 mg/ml of UT-ex, untransformed HaCaT keratinocytes were more resistant than all squamous carcinoma cell lines tested (Fig. 2A–E). Similar results were obtained by treating cells with the extract that was first lyophilized, stored at −20 °C for 1 month and then reconstituted by re-adding water up to the initial volume (reUT-ex) (Fig. S1).

Using MTT assays, we detected an increase of cell viability at UT-ex concentrations ranging between 0.3 and 1.5 mg/ml, in all tested cell lines (Fig. 2A–E). With cell growth profiling, however, we found no increase in the rate of cell proliferation (Fig. S2 A–C).

Next, we focused our further studies on A431 and SCC022 carcinoma cells which are the most sensitive and the most resistant to UT-ex, respectively.

We investigated the effect of low doses of UT-ex (0.3 and 1.5 mg/ml) on cell cycle distribution by flow cytometry. As shown in Fig. 3A, B and C, there was a significant change in the cell number in the different cell cycle phases. Specifically, at 1.5 mg/ml of UT-ex, in HaCaT cells we observed accumulation of G1 arrested cells (3 A) while the majority of A431 and SCC022 cells were arrested in the G2/M phase (Fig. 3B and C). The observed cell cycle arrest was associated with the induction of the cell cycle inhibitor p21/WAF protein (Fig. 3D).

The presence of cleaved Poly [ADP-ribose] polymerase 1 (PARP-1) is used diagnostically to detect apoptosis in many cell types (Gobeil et al., 2001). Thus, we analyzed PARP-1 proteolysis by immunoblot in HaCaT, A431 and SCC022 cells treated with 0.3, 3.0 and 10 mg/ml of UT-ex. Based on the MTT assays, at this concentration range, we expected to detect molecular evidence of UT-ex effects. In fact, at 0.3 mg/ml of UT-ex all cell lines showed a viability comparable to the control cells; at 3.0 mg/ml the most resistant cell line (SCC022) exhibited a clear response to the treatment; finally at 10 mg/ml, all cell lines were sensitive to UT-ex treatment and underwent cell death.

The appearance of the 89 kDa PARP-1 fragment generated by Caspase 3 cleavage (Fig. 4A, black arrows) along with the apoptotic DNA fragmentation pattern observed in UT-ex treated HaCaT cells suggested the occurrence of apoptosis (Fig. 4B). This was also

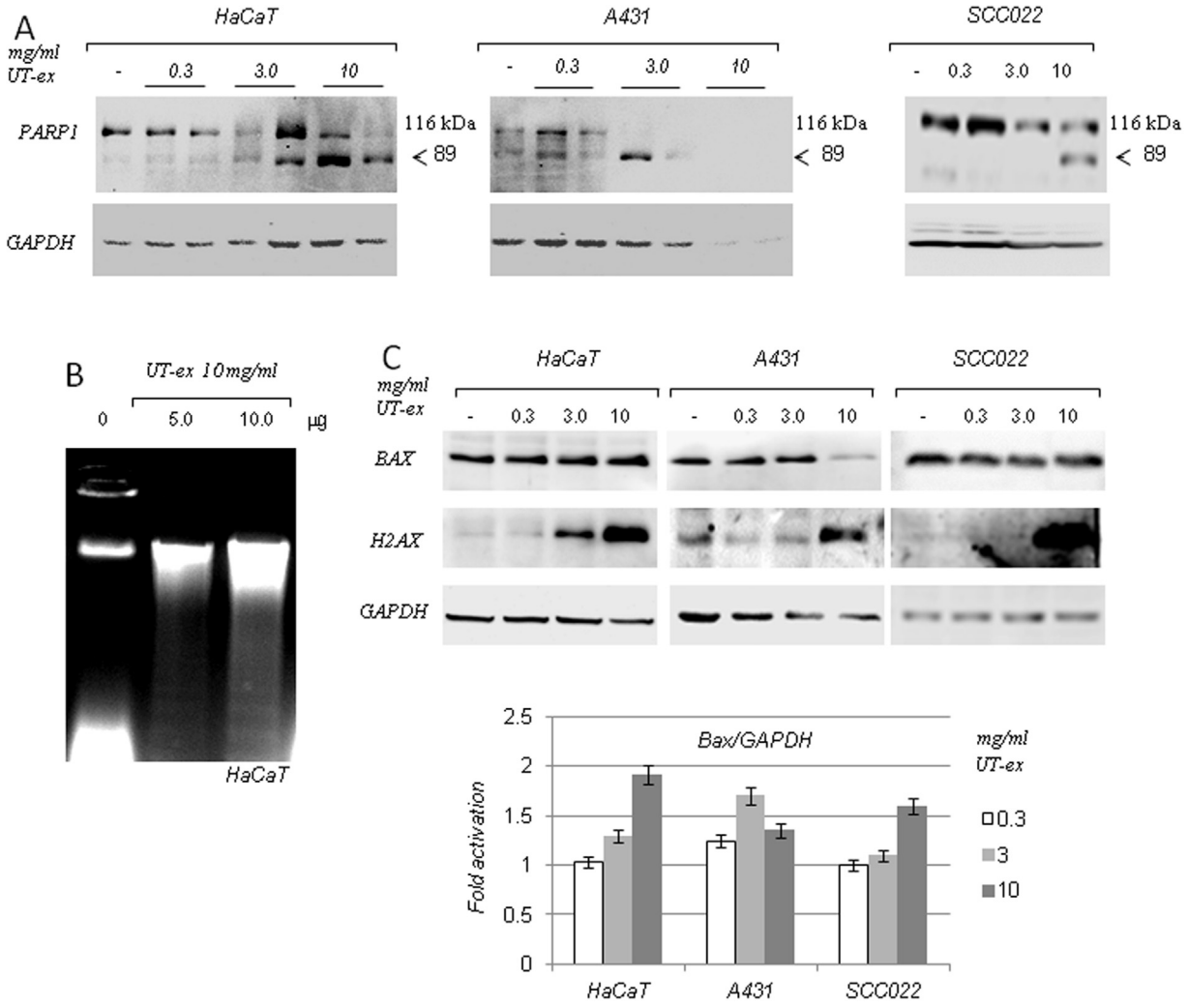

Fig. 4. (**A**) Representative immunoblot analyses of HaCaT, A431 and SCC022 cells after 48 h of treatment with the indicated doses of UT-ex (mg/ml). Equal aliquots of extracts (25 µg) were subjected to immunoblot analysis with PARP1 antibodies. (**B**) Electrophoresis on agarose gel (1.2%) of genomic DNA isolated from HaCaT cells treated or not with 10 mg/ml of UT-ex extract. (**C**) *upper panel* Representative immunoblot analyses of HaCaT, A431 and SCC022 cells after 48 h of treatment with the indicated doses of UT-ex (mg/ml). Equal aliquots of extracts (25 µg) were subjected to immunoblot analysis with Bax and H_2AX antibodies. GAPDH antibodies were used as loading control; *lower panel* Densitometric analysis of Bax protein levels.

confirmed by the comet assay (Fig. S3) and induction of the proapoptotic Bax protein in HaCaT and SCC022 cells (Fig. 4C). Unfortunately, because of their high sensitivity to UT-ex, very limited amount of cell extract was recovered from A431 cells treated with 10 mg/ml of UT-ex. However, the strong induction of γ-H2AX histone protein indicated the occurrence of DNA damage in all tested cell lines (Fig. 4C).

3.2. UT-ex induces oxidative stress in HaCaT and A431 cells

Previous studies have shown that many natural products cause apoptosis in cancer cells through the production of Reactive Oxygen Species (ROS) (Martin-Cordero et al., 2012). Therefore, we tested whether apoptosis induced by UT-ex was ROS-dependent using flow cytometry after staining with 2′−7′ diclorofluorescin diacetate (DCFDA). Control cells were incubated for 30 min with DCFDA alone, while treated cells were incubated with UT-ex (0.3 or 3.0 mg/ml) for 24 h and subsequently with DCFDA for 30 min. The amount of ROS was normalized for a sample of cells without DCFA. Compared to control cells, HaCaT and A431 cells treated with 0.3 mg/ml of UT-ex showed a moderate increase of intracellular ROS (Fig. 5). Treatment with 3 mg/ml of UT-ex, instead, resulted in a 28% and 70% increase in ROS production in HaCaT and A431 cells, respectively (Fig. 5). These results strongly suggest that the observed cell death was ROS-dependent.

3.3. UT-ex influences YB-1 proteolytic cleavage

The multifunctional Y-box binding Protein-1 (YB-1 or YBX-1) provides cellular protection from oxidative stress and participates in DNA damage repair mechanisms by interacting with Mre11 and Rad50 complexes (Somasekharan et al., 2015; Kim et al., 2013). It was previously reported that YB-1 cleavage by the 20 S proteasome leads to the accumulation of a 36 kDa nuclear form which is recruited to DNA damage sites to participate in DNA repair (Kim et al., 2013).

We tested the effect of increasing the amount of UT-ex (from 0.3 to 10 mg/ml) on YB-1 using immunoblot analyses.

In untreated HaCaT cells, full length YB-1 (50 kDa) was largely predominant over the 36 kDa form (Fig. 6A, lane 1). However, the 36 kDa proteolytic fragment of YB-1 increased as a result of UT-ex treatment up to 3.0 mg/ml (Fig. 6A, lanes 2–5) and abruptly disappeared at 10 mg/ml of UT-ex (Fig. 6A, lane 6 and 7). Interestingly, in untreated SCC022 and A431 cells, the 50 and 36 kDa forms of YB-1 were almost equally represented in (Fig. 6B and C, lanes 1). However, similarly to what we observed in HaCaT, in SCC022 cells the 36 kDa

Intracellular ROS levels

Cell type	- DCFA	+ DCFA	DCFA+ 0.3 UT-ex	DCFA+ 3.0 UT-ex
HaCaT	1	1.6%	2.3%	28%
A431	1	1.2%	3.2%	70%

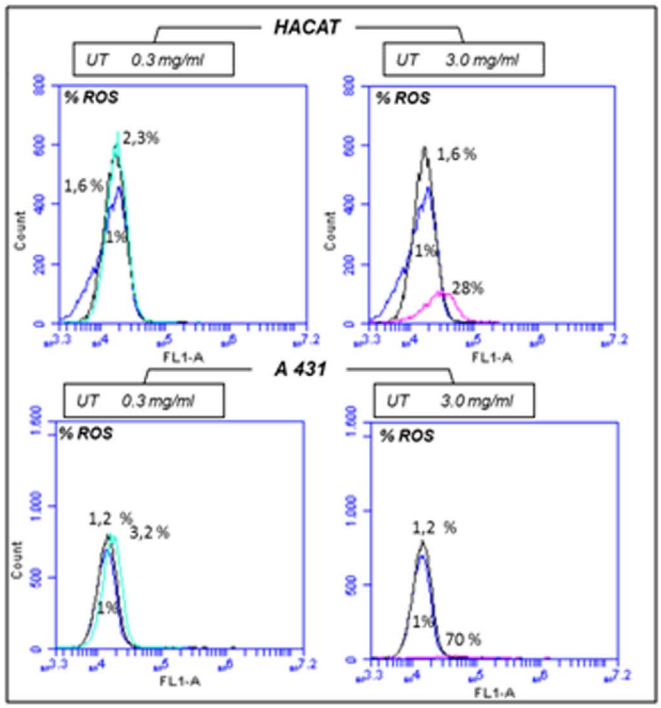

Fig. 5. Percentage of intracellular ROS levels in HaCaT and A431 cells treated with 0.3 or 3.0 mg/ml UT-ex. Data were analyzed and converted in percentage of ROS by BD Accuri C6 Software. Representative FACS-derived histograms showing increased ROS in HaCaT (upper panel) and A431 (lower panel) cells treated with UT-ex 0.3 mg/ml (left panel) or UT-ex 3.0 mg/ml (right panel) compared with control cells without DCFDA (% of ROS = 1) and untreated cells incubated with DCFDA. 20.000 events were evaluated. Data were analyzed and converted in percentage of ROS by BD Accuri C6 Software.

band of YB-1 was significantly reduced at 10 mg/ml of UT-ex (Fig. 6B, lane 4). In A431 cells, however, the 36 kDa YB-1 band disappeared in cells treated with 3.0 mg/ml of UT-ex (Fig. 6C, lanes 3 and 5). In contrast, the level of full length YB-1 appeared to be unaffected or even increased thereby suggesting that full length YB-1 was stabilized (Fig. 6A, B, C). However, it has to be noted that at 10 mg/ml of UT-ex both YB-1 and GAPDH were undetectable because of extensive cell death (Fig. 6C, lane 6). Strikingly, the level of hnRNPA1, a RNA-binding protein that is known to be degraded by caspase 3 (Back et al., 2002), was completely degraded in cells treated with UT-ex, in a dose-dependent manner (Fig. 6D, E and F).

We have previously shown that YB-1 is polyubiquitinated (Di Martino et al., 2016). Moreover, under DNA damage conditions, YB-1 undergoes a proteasome-dependent proteolytic cleavage, resulting in the YB-1 36 kDa form. Accumulation of full length YB-1, with the parallel disappearance of the YB-1 36 kDa, suggests an impairment of proteasome activity. Therefore, we investigated whether UT-ex caused an accumulation of protein ubiquitination. Immunoblot analysis of total protein extract from untreated and UT-ex treated cells clearly showed an increase of total ubi-conjugated proteins, thereby confirming a defective proteasomal degradation in the presence of UT-ex (Fig. 7A, B, C). Finally, we performed a specific immunoprecipitation of YB-1 protein. YB-1 immunocomplexes were then analyzed by immunoblot with Ubiquitin (Ubi) antibodies. As shown in Fig. 7D, the signal obtained from cells treated with UT-ex was enhanced, thus confirming that Ubi-conjugated YB-1 was accumulated (Fig. 7D).

3.4. Preliminary chemical analysis of aqueous extract

The dried aqueous extract obtained from *Uncaria tomentosa* cell cultures was analyzed by TLC in different solvent mixtures: *i*-PrOH:H_2O 8:2, v/v; $CHCl_3$:*i*-PrOH 9:1, v/v; EtOAc:*n*-hexane 6:4, v/v that showed the presence of a mixtures of low and medium molecular weight compounds. The extract was dissolved in a minimal amount of ultrapure Milli-Q water and dialysed (cut-off 3500 Da). The tube content (IN) and the out fraction (OUT) were collected lyophilized, and re-suspended in the same initial volume. The fractions were separately tested for their cytotoxic activity against A431 cells by MTT assay as previously described. Remarkably, most of cytotoxic activity remained in the OUT fraction that contains hydrophilic low molecular weight metabolites (Fig. S4). Therefore, the OUT fraction was analyzed by HPLC, ^{1}H NMR and LC-TOF.

The HPLC profile of the OUT fraction of the dialyses (Fig. S5) showed the presence of several peaks. Its ^{1}H NMR (Fig. S6) showed the presence of two main anomeric protons at δ 5.4 and 5.1 ppm and complex signals in the region of the hydroxylated protons in the range of δ 4.1–3.2 ppm, suggesting the presence of saccharide mixtures. Complex signals were also present in the region of aliphatic protons at δ 2.0–1.5 ppm (Pretsch et al., 2000).

The LC-MS/TOF (Figs. S7 and 8) spectra showed eight main peaks detected in the molecular weight range of 350–570 *m/z* that could be consistent with the nature of metabolites suggested by HPLC and ^{1}H NMR analysis. In particular, four of them (Fig. S7) showed both the sodiated $[M + Na]^+$ and the sodiated dimmer $[2\,M + Na]^+$ forms at *m/z* 383 and 743, 409 and 795, 428 and 833, 501 and 979, consistent with molecular weight of 360, 386, 405 and 478, respectively.

4. Discussion

Biological effects of complex mixtures of phytochemicals are difficult to predict from chemical analysis of individual constituents because they generally combine the advantage of targeting multiple molecular pathways that are involved in complex disorders with a considerable reduction in toxic side effects (Wagner et al., 1985b).

Cancer control may benefit from the potential in alternative therapies. Ideally, a phytochemical should possess anti-tumor properties, minimal, toxicity and a defined mechanism of action. The knowledge of the mechanism of action and the signaling pathways targeted by natural compounds can lead to understanding the molecular mechanisms involved in cancer progression and may indicate novel therapeutic approaches.

Induction of apoptosis is considered one of the most important markers of cytotoxicity for antitumor agents. Some natural compounds, including plant metabolites, are able to induce apoptotic pathways that, through various mechanisms are usually blocked in cancer cells.

We have presented evidence that an aqueous extract from *Uncaria tomentosa* barks affects viability of squamous carcinoma cells through a combination of *increased oxidative stress* and *impaired DNA repair*. Our data are in agreement with previous studies showing that *Uncaria tomentosa* extract is able to enhance chemotherapy-induced apoptosis, with an increase in caspase activities and DNA fragments in cultures of neoplastic cells (De Oliveira et al., 2014).

In our study, *Uncaria tomentosa* water extract exhibited dose-dependent cytotoxic and antimitotic effects on human spontaneously immortalized HaCaT keratinocytes and squamous carcinoma cells. The inhibitory effect on cell viability was time and dose-dependent.

Remarkably, compared to the other tumor cell lines used in this study, the SCC022 cells exhibit a very different response to UT-ex treatment. However, in a previous work from our group (Troiano et al.,

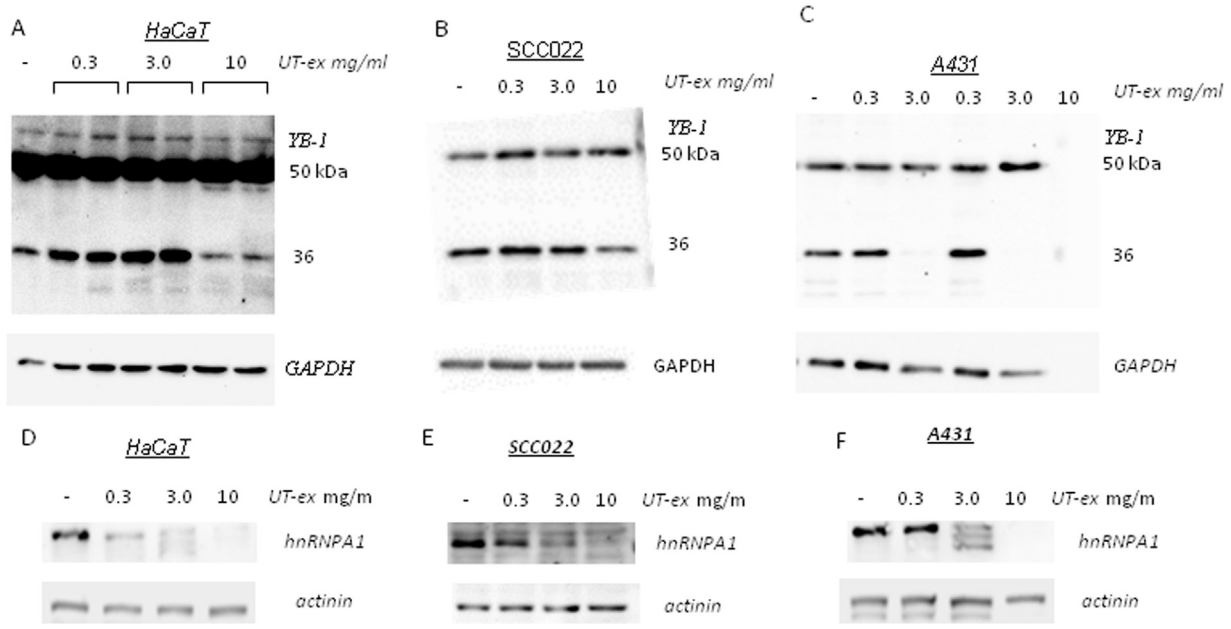

Fig. 6. (A–C) Immunoblot analysis of HaCaT, SCC022 and A431 cells treated with 0.3, 3.0 and 10 mg/ml of UT-ex for 48 h. Equal aliquots of extracts (25 μg) were loaded and subjected to SDS-PAGE and immunoblot analysis with YB-1 antibodies. GAPDH antibodies were used as loading control. **(D-F)** Immunoblot analysis of HaCaT, SCC022 and A431 cells treated with 0.3 and 3.0 and 10 mg/ml of UT-ex for 48 h. Equal aliquots of extracts (25 μg) were loaded and subjected to SDS-PAGE and immunoblot analysis with hnRNPA1 antibodies. Actinin antibodies were used as loading control.

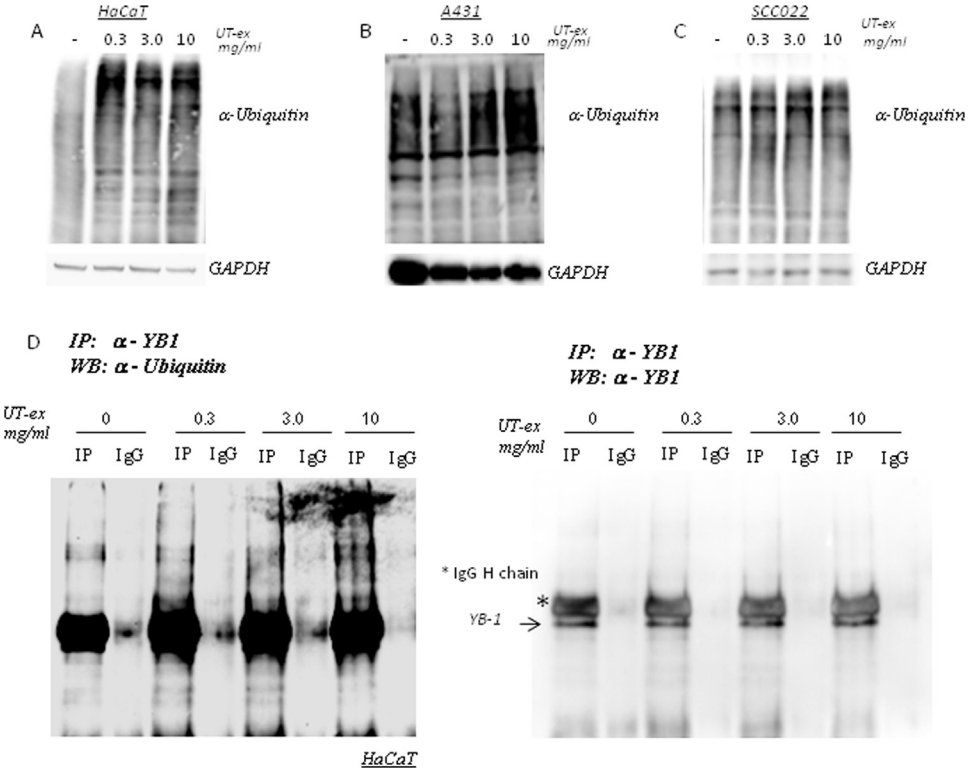

Fig. 7. (A–C) Immunoblot analysis of HaCaT, A431 and SCC022 cells treated with 0.3, 3.0 and 10 mg/ml of UT-ex for 48 h. Equal aliquots of extracts (25 μg) were loaded and subjected to SDS-PAGE and immunoblot analysis with Ubiquitin antibodies. GAPDH antibodies were used as loading control. **(D)** Equal aliquots of HaCaT cells treated with 0.3 and 3.0 and 10 mg/ml of UT-ex for 48 h shown in Fig. 7A were immunoprecipitated (**IP**) with anti-YB-1 or an irrelevant α-rabbit antibodies (IgG). Immunocomplexes were blotted and probed with Ubiquitin (left panel) or YB-1 (right panel) antibodies.

2015) we have shown that this cell line is PTEN-defective and therefore exhibits constitutive AKT_{Ser473} hyperphosphorylation that was even potentiated by YB-1 silencing. Constitutive activation of AKT survival pathway may be the likely explanation for the lower sensitivity of these cells to UT-ex treatment.

Morphological changes induced by UT-ex were associated with PARP1 cleavage, increase of BAX protein levels, and internucleosomal DNA fragmentation indicating apoptosis.

An important finding of our work is that Uncaria-induced cytotoxicity was associated with ROS production. ROS are also a by-product of normal metabolism; short exposure of non-proliferating cells to relatively low doses of ROS was shown to activate signal transduction pathways comparable to the effects of mitogens (Deavall et al., 2012). This may be the most likely explanation for the increase of cell viability observed at low concentrations of UT-ex, in the majority of the cell lines tested in this work (HaCaT and SCCs). However, when the level of ROS exceeded the cellular antioxidant capacity, their reactive nature may otherwise cause damage to key cellular components and induce cell

death.

Because cancer cells are sensitive to oxidative stress, the mechanism of action for many cancer chemotherapeutic drugs involves ROS-mediated apoptosis (De Oliveira et al., 2014). Interestingly, after treatment with low doses of UT-ex, immortalized keratinocytes were still able to activate a G1/S cell cycle checkpoint, allowing them to repair DNA damage before DNA duplication. This could potentially explain their relative resistance to UT-ex induced apoptosis. Under the same conditions, A431 and SCC022 cancer cells showed a defective G1/S checkpoint with a consequent accumulation of G2/M arrested cells followed by massive apoptosis.

Exposure of non-proliferating cells to relatively low doses of ROS can activate mitogenic signals (Deavall et al., 2012). At low doses, UT-ex increased HaCaT and A431 cell viability; however, we found no significant increase in the rate of cell proliferation, thereby suggesting that, at the concentration tested, UT-ex could enhance cell metabolism rather than cell proliferation.

Our in vitro studies implicate the Y-Box-binding protein 1 (YB-1) in UT-ex induced apoptosis. YB-1 is a multifunctional protein participating in oncogenesis and is an oncomarker of breast, lung, liver, ovarian and squamous cell carcinoma (Lasham et al., 2013). We have previously identified YB-1 as a partner of ΔNp63α, the predominant protein expressed in proliferative squamous epithelia, and demonstrated that YB-1 and ΔNp63α interplay supports keratinocyte proliferation and protects keratinocytes from apoptosis under genotoxic stress (Di Martino et al., 2016; Di Costanzo et al., 2012). YB-1 is predominantly localized to cytoplasm, where it serves as a sensor of oxidative stress. Indeed, it was found to be implicated in translational repression and assembly of Stress Granules upon heat shock and oxidative stress (Kedersha et al., 2005). However, in response to severe genotoxic insults, UV, doxorubicin, cisplatin, etoposide and prolonged oxidative stress, YB-1 accumulates into the nucleus and participates in DNA damage repair (Kim et al., 2013). In particular, full length YB-1 (50 kDa) undergoes specific post-translational modifications and limited cleavage by the proteasome leading to the nuclear accumulation of the N-terminal YB-1 36 kDa fragment. YB-1 36 kDa form functionally interacts with BER factors (NEIL1, PARP1 and 2) and Double Strand Break (DSB) repair proteins MRE11 and Rad50 (Alemasova et al., 2016) and enhances cell survival (Kim et al., 2013). We believe that the relevance of this mechanism in cancer-cell chemo-resistance is still underestimated.

Strikingly, we found that treatment of cells with lethal doses of UT-ex were associated with the reduction/disappearance of the pro-survival YB-1 36 kDa form in HaCaT, SCC022 and A431 cells. Because the level of full length YB-1 was unaffected, or even increased, by UT-ex treatment, we postulate that UT-ex could have a proteasome-inhibitory activity. The increase of total protein ubiquitination and the accumulation of Ubiquitin-conjugated YB-1 confirmed our hypothesis. It is not hard to speculate that other proteasome inhibitors already in clinical practice such as Bortezomib (Crawford et al., 2011) can exert their anticancer effects by targeting YB-1, and their relative efficacy may partly depend upon on their effect on YB-1 proteolytic cleavage. Although not exhaustive, chemical analysis of UT-ex showed that beside a large amount of saccharides, it contained further low molecular weight metabolites. Previously, phytochemical investigations on *U. tomentosa* and related species suggested the presence of indole and oxindole alkaloids, triterpenes and polyphenols (Lock et al., 2016). However, further purification of the mixture is in progress in order to confirm the nature of these classes of compounds and identify those that are effective against squamous carcinoma cells.

5. Conclusion

Being at the interface between oxidative stress and molecular mechanisms controlling cell proliferation and DNA damage repair, the YB-1 protein might not only provide a survival advantage to error-prone cancer cells, but also protect them from chemotherapy-induced apoptosis. We have clear evidence that *Uncaria tomentosa* water extracts contains bioactive molecules that interfere with the proteasome-mediated YB-1 proteolytic cleavage thus reducing the capacity of cells to effectively repair damaged DNA. Our study indicates that *Uncaria Tomentosa* pro-apoptotic activity results from its ability to simultaneously induce oxidative DNA damage and antagonize the mechanisms of DNA repair relying on the activity of YB-1 36 kDa form. In light of our current knowledge about the pro-apoptotic effects of UT-ex in squamous cancer cells, we believe that this plant may have a high potential value as an effective agent for treatment of cancerous skin lesions.

Acknowledgments

We thank the company BIOPHARMA s.r.l. for constructive collaboration.

Funding

This work was supported by Regione Campania LR No 5/2007, Progetto DIMO POR-FESR Campania 2007–2013 Bando per la realizzazione delle reti biotecnologiche Campane and Programma Ricerca e Innovazione Smart Specialization Strategy (RIS3) Regione Campania.

Conflict of interest statement

None declared.

Appendix A. Supplementary material

Supplementary data associated with this article can be found in the online version at http://dx.doi.org/10.1016/j.jep.2017.09.031.

References

Akesson, C., Lindgren, H., Pero, R.W., Leanderson, T., Ivars, F., 2003. An extract of Uncaria tomentosa inhibiting cell division and NF-kappa B activity without inducing cell death. Int. Immunopharmacol. 3, 1889–1900.

Alemasova, E.E., Moor, N.A., Naumenko, K.N., Sukhanova, M.V., Pestryakov, P.E., Lavrik, O.I., 2016. Y-box-binding protein 1 as a non-canonical factor of base-excision repair. Biochim. Biophys. Acta 1864 (12), 1631–1640.

Amoresano, A., Di Costanzo, A., Leo, G., Di Cunto, F., La Mantia, G., Guerrini, L., Calabrò, V., 2010. Identification of ΔNp63α protein interactions by mass spectometry. J. Proteome Res. 9 (4), 2042–2048.

Back, S.H., Shin, S., Jang, S.K., 2002. Polypirimidine tract-binding proteins are cleaved by Caspase-3 during apoptosis. J. Biol. Chem. 277, 27200–27209.

Boukamp, P., 2005. Non-melanoma skin cancer: what drives tumor development and progression. Carcinogenesis 26, 1657–1667.

Calabrò, V., Mansueto, G., Santoro, R., Gentilella, Pollice, A., Ghioni, P., Guerrini, L., La Mantia, G., 2004. Inhibition of p63 transcriptional activity by p14ARF: functional and physical link between human ARF tumor suppressor and a member of the p53 family. Mol. Cell. Biol. 24, 8529–8540.

Ccahuana-Vasquez, R.A., Santos, S.S.F., Koga-Ito, C.Y., Jorge, A.O.C., 2007. Antimicrobial activity of Uncaria tomentosa against oral human pathogens. Braz. Oral. Res. 21 (1) (Dx.doi.org/10.1590).

Crawford, L.J., Walker, B., Irvine, A.E., 2011. Proteasome inhibitors in cancer therapy. J. Cell Commun. Signal. 5 (2), 101–110.

De Oliveira, L.Z., Farias, I.L.G., Rigo, M.L., et al., 2014. Effect of uncaria tomentosa extract on apoptosis triggered by oxaliplatin exposure on HT29 cells. Evid.-Based Complement. Altern. Med.: eCAM 2014, 274786. http://dx.doi.org/10.1155/2014/274786.uld.

Deavall, D.G., Martin, E.A., Horner, J.M., 2012. Drug-induced oxidative stress and toxicity. J. Toxicol. 2012, 1–13.

Di Costanzo, A., Festa, L., Roscigno, G., Vivo, M., Pollice, A., Morasso, M., La Mantia, G., Calabrò, V., 2011. A dominant mutation etiologic for human tricho-dento-osseous syndrome impairs the ability of DLX3 to downregulate ΔNp63α. J. Cell. Physiol. 226 (8), 2189–2197.

Di Costanzo, A., Troiano, A., Di Martino, O., Cacace, A., Natale, C.F., Ventre, M., Netti, P., Caserta, S., Pollice, A., La Mantia, G., Calabrò, V., 2012. The p63 protein isoforms ΔNp63α modulates Y-box binding protein 1 in its subcellular distribution and regulation of cell survival and motility genes. J. Biol. Chem. 287 (36), 30170–30180.

Di Martino, O., Troiano, A., Guarino, A.M., Pollice, A., Vivo, M., La Mantia, G., Calabrò, V., 2016. . ΔNp63α controls YB-1 protein stability: evidence on YB-1 as a new player in keratinocyte differentiation. Genes Cells 21, 648–660. http://dx.doi.org/10.1111/gtc.12373.

Garcia Prado, E., Garcia Gimenez, M.D., De la Puerta Vazquez, R., 2007. Antiproliferative effects of mitraphylline, a pentacyclic oxindole alkaloid of Uncaria tomentosa on human glioma and neuroblastoma cell lines. Phytomedicine 14, 280–284.
Gobeil, S., Boucher, C.C., Nadeau, D., Poirier, G.G., 2001. Characterization of the necrotic cleavage of poly(ADP-ribose) polymerase (PARP-1): implication of lysosomal proteases. Cell Death Differ. 8 (6), 588–594.
Gurrola-Diaz, C.M., Garcia-Lopez, P.M., Gulewicz, K., Pilarski, R., Dihlmann, S., 2011. Inhibitory mechanisms of two Uncaria tomentosa extracts affecting the Wnt-signaling pathway. Phytomedecine 18 (8–9), 683–690.
Heitzman, M.E., Neto, C.C., Winiarz, E., Vaisberg, A.J., Hammond, G.B., 2005. Ethnobotany, phytochemistry and pharmacology of Uncaria Rubiaceae. Phytochemistry 66, 5–29.
Kaiser, S., Dietrich, F., de Resende, P.E., Verza, S.G., Moraes, R.C., Morrone, F.B., Batastini, A.M., Ortega, G.G., 2013. Cat´s claw oxindole alkaloid isomerization induced by cell incubation and cytotoxic activity against T24 and RT4 human bladder cancer cell lines. Planta Med. 79, 1413–1420.
Kedersha, N., Stoecklin, G., Ayodele, M., Yacono, P., Lykke-Andersen, J., Fritzler, M.J., Scheuner, D., Kaufman, R.J., Golan, D.E., Anderson, P., 2005. Stress granules and processing bodies are dynamically linked sites of mRNP remodeling. J. Cell Biol. 169 (6), 871–884.
Keplinger, K., Laus, G., Wurm, M., Dierich, F., Teppner, H., 1998. Uncaria tomentosa (Wild) DC. – ethnomedicinal use and new pharmacological, toxicological and botanical results. J. Ethnopharmacol. 64 (1), 23–33.
Kim, E.R., Selyutina, A.A., Buldakov, I.A., Evdokimova, V., Ovchinnikov, L.P., Sorokin, A.V., 2013. The proteolytic YB-1 fragment interacts with DNA repair machinery and enhances survival during DNA damaging stress. Cell Cycle 12, 3791–3803.
Lasham, A., Print, C.G., Dunn, S.E., Braithwaite, A.W., 2013. YB-1 oncoprotein, prognostic marker and therapeutic target? Biochem. J. 449, 11–23.
Lo Iacono, M., Di Costanzo, A., Calogero, R.A., Mansueto, G., Saviozzi, S., Crispi, S., Pollice, A., La Mantia, G., Calabrò, V., 2006. The hay wells syndrome-derived TAp63αQ540L mutant has impaired transcriptional and cell growth regulatory activity. Cell Cycle 5 (1), 78–87.
Lock, O., Perez, E., Villar, M., Flores, D., Rojas, R., 2016. Bioactive compounds from plants used in peruvian traditional medicine. Nat. Prod. Comm. 11 (3), 315–337.
Mammone, T., Akesson, C., Gan, D., Giampapa, V., Pero, R.W., 2006. A water soluble extract from Uncaria tomentosa (Cat Claw's) is a potent enhancer of DNA repair in primary organ cultures of human skin. Phytother. Res. 20 (3), 178–183.
Martin-Cordero, C., Martin-Cordero, C., Leon-Gonzalez, A.J., Calderon-Montano, J.M., Burgos-Moron, E., Lopez-Lazaro, M., 2012. Pro-oxidant natural products as anticancer agents. Curr. Drug Targets 13 (8), 1006–1028.
Mentor, J.M., Etemadi, A., Patta, A.M., Scheinfeld, N., 2015. Topical AC-11 abates actinic keratoses and early squaous cell cancers in hairless mice exposed to Ultraviolet A (UVA) radiation. Dermatol. Online J. 21 (4) (pii:13030/qt5rt46141).
Pretsch, E., Buhlmann, P., Affolter, C., 2000. Structure Determination of Organic Compounds – Tables of Spectral Data, 3rd ed. Springer-Verlag, Berlin, pp. 161–243.
Resto, V.A., Burdick, M.M., Dagia, N.M., McCammon, S.D., Fennewald, S.M., Sackstein, R., 2008. L-selectin-mediated lymphocyte-cancer cell interactions under low fluid shear conditions. J. Biol. Chem. 283 (23), 15816–15824.
Riva, L., Coradini, D., Di Fronzo, G., De Feo, V., De Tommasi, N., De Simone, F., Pizza, C., 2001. The antiproliferative effects of Uncaria tomentosa extracts and fractions on the growth of breast cancer cell line. Anticancer Res. 21 (4A), 2457–2461.
Sapijaszko, M., Zloty, D., Bourcier, M., Poulin, Y., Janiszewski, P., Ashkenas, J., 2015. Non-melanoma skin cancer in Canada chapter 5: management of squamous cell carcinoma. J. Cutan. Med. Surg. 19, 249–259.
Somasekharan, S.P., El-Naggar, A., Leprivier, G., Cheng, H., Hajee, S., Grunewald, T.G., Zhang, F., Ng, T., Delattre, O., Evdokimova, V., Wang, Y., Gleave, M., Sorensen, P.H., 2015. YB-1 regulates stress granule formation and tumor progression by translationally activating G3BP1. J. Cell Biol. 208, 913–929.
Troiano, A., Lomoriello, I.S., di Martino, O., et al., 2015. Y-box binding protein 1 is part of a complex molecular network linking ΔNp63α to the PI3K/Akt pathway in cutaneous squamous cell carcinoma. J. Cell. Physiol. 2015, 2067–2074.
Wagner, H., Kreutzkamp, B., Jurcic, K., 1985a. The alkaloids of Uncaria tomentosa and their phagocytosis-stimulating action. Planta Med. 5, 419–423.
Wagner, H., Kreutskamp, B., Jurcic, K., 1985b. Die Alkaloide von Uncaria tomentosa und ihre Phagozytose-steigernde Wirkung. Planta Med. 51 (5), 419–423.